Limited warming of Middle Miocene arid low-latitude climates: application of clumped isotopes in sabkha environments.

Marta Marchegiano[1], Martin Ziegler[2], Or M. Bialik[3], David De Vleeschouwer[3]

1 *Departamento de Estratigrafía y Paleontología, Universidad de Granada, 18071 Granada, Españ, martamarchegiano@ugr.es*

2 Department of Earth Sciences, Utrecht University, Utrecht, 3584 CB, the Netherland, M.Ziegler@uu.nl

3 Institute of Geology and Palaeontology, University of Münster, Münster, German, obialik@uni-muenster.de, ddevlees@uni-muenster.de

**corresponding author, Marta Marchegiano, martamarchegiano@ugr.es*

Limited warming of Middle Miocene arid low-latitude climates: application of clumped isotopes in sabkha environments.

Marta Marchegiano[1], Martin Ziegler[2], Or M. Bialik[3], David De Vleeschouwer[3]

1 *Departamento de Estratigrafía y Paleontología, Universidad de Granada, 18071 Granada, Españ, martamarchegiano@ugr.es*

2 *Department of Earth Sciences, Utrecht University, Utrecht, 3584 CB, the Netherland, M.Ziegler@uu.nl*

3 *Institute of Geology and Palaeontology, University of Münster, Münster, German, obialik@uni-muenster.de, ddevlees@uni-muenster.de*

**corresponding author, Marta Marchegiano, martamarchegiano@ugr.es*

ABSTRACT

Reconstructing past climatic conditions in arid and hot environments is challenging due to a scarcity of climate archives. However, this task is crucial for assessing the sensitivity of these areas to climate change. The lack of reliable proxies currently prevents precise and absolute temperature and moisture reconstructions. Clumped isotopes on sabkha calcite might alleviate this situation. In this study, we apply the clumped isotope technique (Δ_{47}) to both modern and Middle Miocene fossil sabkha samples and we report temperatures between 26.2±5.4 to 33.6±6.3ºC. Our results suggest that sabkha calcite-aragonite minerals primarily reflect summer half-year temperatures, corresponding to the dry season when most calcite-aragonite precipitation occurs in these environments. Reconstructed $\delta^{18}O_{water}$ values range between 3.2±0.9 and 5.3±0.8‰, scaling with the intensity of evaporation in these intertidal, supratidal and lagoonal settings. Despite higher atmospheric CO_2 levels during the Middle Miocene, reconstructed temperatures are similar to modern ones, suggesting a reduced climate sensitivity

at low latitude. Overall, sabkha clumped isotopes offer a valuable tool for bridging the latitudinal gap in continental paleotemperature reconstructions near the horse latitudes.

INTRODUCTION

The high latitudes cool and warm markedly more rapidly than the low latitudes under the influence of global climate change. This phenomenon was dubbed "Polar Amplification" by Budyko (1969). The amplification of high-latitude climate change is often associated with changes in albedo due to loss of ice and snow coverage (Kirtman et al., 2014). But the gradient is also sustained by the separation of air circulation between the high and lower latitudes by the jet stream, which degrades under a lower latitudinal gradient (Stendel et al., 2021). Warming in the lower latitudes thus exerts a feedback mechanism through a more efficient latitudinal redistribution of heat. Yet, the limited knowledge on the response of low-latitude climates to global warming is hampering a full quantification of this feedback mechanism. This knowledge gap is chiefly caused by a combination of under-sampling and a limited availability of climate archives in hot and dry environments (Nelson et al., 2023). Moreover, our current ability to reconstruct continental paleotemperatures in semi-arid environments is also hindered by the lack of reliable proxies in potential climate archives.

While terrestrial carbonate archives in arid and hot regions are rare due to precipitation scarcity and the absence of large water bodies, sabkha environments might contain useful paleoclimate indicators. Sabkha denotes a coastal, supratidal or upper intertidal mudflat or sandflat shaped by semiarid to arid climates, where evaporitic minerals such as gypsum, halite, anhydrite and calcite accumulate (Warren and Kendall, 1985). Today, they are found at the horse latitudes (i.e., between ca. 30 and 35 degrees north and south of the equator) but looking back in geologic history, these regions may have covered a larger land surface area. Here, we highlight the potential of carbonate-bearing sediments, accumulated in sabkha environments, as unique archives to reconstruct past atmospheric conditions: specifically, dry-season air temperature. Paleoclimate data extracted from sabkha deposits can thus enhance paleoclimate reconstructions within the horse latitudes, while also facilitate more comprehensive comparisons between proxy data and general circulation model (GCM) outputs.

The assimilation of paleoclimate reconstructions from proxies and climate models provides a mean to bring down uncertainties (Judd et al., 2024). The Miocene is an epoch of global warmth with CO_2 concentrations ranging from 300 to 600 ppm (Sosdian et al., 2018). Previous proxy-based Miocene paleoclimate studies have already suggested a less pronounced latitudinal temperature gradient (Steinthorsdottir et al. 2020). Yet, in order to validate climate modelling, it is crucial to have more abundant and especially accurate absolute temperature reconstructions.

Carbonate clumped-isotopes (Δ_{47}) are useful to reconstruct paleotemperatures and hydrologic conditions in both marine and terrestrial archives (Eiler, 2007). The abundance of ^{13}C–^{18}O bonds within carbonate minerals is temperature-dependent and independent of the isotopic composition of the water if which the carbonate formed. If carbonates precipitated at isotopic equilibrium, unified Δ_{47} calibrations can be used to calculate absolute water temperatures (Anderson et al., 2021 and Daëron and Vermeesch, 2024), as well as to reconstruct the isotopic composition of the water ($\delta^{18}O_w$). Non-equilibrium carbonate can be detected with and corrected for with additional Δ_{48} measurements (Fiebig et al., 2021)

To date, sabkha carbonates have been employed for clumped-isotope paleothermometry in only a handful of studies. These studies primarily pertain to the reconstruction of burial histories and dolomitization, yielding first indications that evaporitic carbonates precipitate at equilibrium (Bergmann et al., 2018, Sena et al., 2014, Abbott et al., 2013). However, the timing of carbonate precipitation, and consequently the temperature recorded by sabkha sediments remain open questions that are fundamental to the use of sabkha as a paleoclimatic indicator. Here, we present new Δ_{47} analyses from modern sabkha carbonates (Yas Lagoon, United Arab Emirates) and Miocene sabkha carbonates (IODP Hole U1464C, North West Australian Shelf). These results corroborate earlier findings (Bergmann et al., 2018, Sena et al., 2014, Abbott et al., 2013) that sabkha calcite precipitate at equilibrium and seem to suggest that sabkha clumped isotope temperatures represent summer half-year temperatures in these hot and arid environments. Reconstructed middle-Miocene temperatures confirm a lower climate amplification at low latitude and average summer half-year temperature close to the present ones.

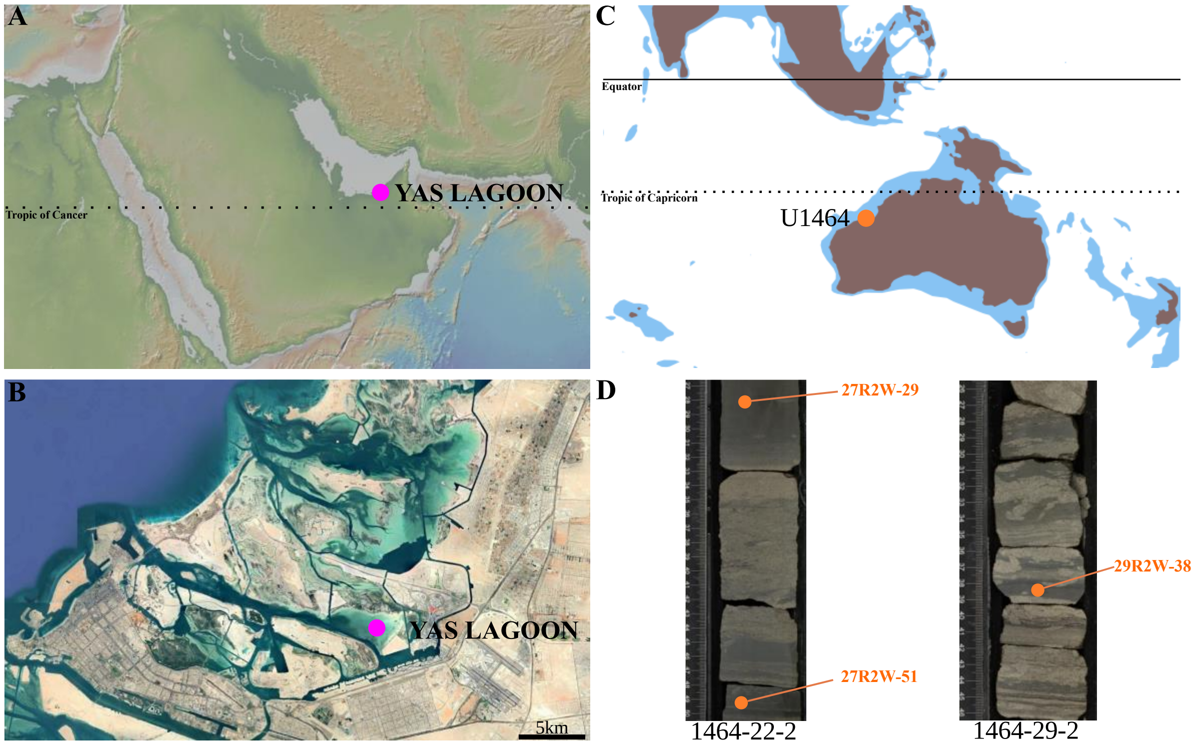

Figure 1: Geographical position of the collected samples: A, B, in Yas lagoon (Abu Dhabi, United Arab Emirate) (A, map modified from GeoMapApp 3.7.2 http://www.geomapapp.org and Ryan et al., 2009) C, of the U1464 core from the IODP expedition 365 (North West Australian Shelf) (Middle Miocene map from Kocsis & Scotese, 2023). In D pictures of the U1464 core and sampling locations.

MATERIALS AND METHODS

Sabkha samples

Miocene Sabkha – North West Australian Shelf

Three fossil sabkha samples come from International Ocean Discovery Program (IODP) Site U1464 (18°04′S, 118°38′E, Roebuck Basin), cored at a present-day water depth of 270 m water depth (Gallagher et al., 2015). Middle and Late Miocene sediments were deposited in a shallow-marine and, possibly, subaerial environment. The latter is characterized by tide-laminated sediments and evaporitic nodules that indicate arid conditions (Groeneveld et al., 2017). Laminated organic-rich layers, gypsum nodules, and anhydrite nodules with chickenwire textures delineate the most arid sabkha-like interval of the succession (Groeneveld et al., 2017). Here, we analyze three samples from this interval (571.2, 552.49 and 552.28 mbsf, ~12 - 13 Ma). These samples were previously mineralogically investigated by Petrick et al. (2019).

Modern Sabkha - Yas Lagoon

Modern sabkha samples were collected in the Yas Lagoon (24º30'N 54º36'E) in Abu Dhabi from the sabkha's algal mat surface (Figure 1). The lagoon is connected to the Persian Gulf by tidal channels and does not have a riverine influx, however, seasonal floods have been observed (Terry et al., 2023). The area experiences semi-diurnal tidal cycles, resulting in two high tides and two low tides daily, with a tidal range of 1–2 meters (Pederson et al., 2021). Yas Lagoon is a highly restricted inner lagoon with a salinity range from 42 to 48‰, a mean pH of 8.05, seawater $\delta^{13}C_{DIC}$ between 1 and -2‰, and $\delta^{18}O_W$ between 2.2 and 3.7‰ during winter (Pederson et al., 2021) while during summer $\delta^{18}O_W$ can reach values of 5.36‰ (Mckenzie, 1980). Because of the high evaporation rate during spring-summer, these parameters are expected to be highly variable during the year. The present-day climate of the area is summarized in Figure 2 and described in Lokier & Fiorini (2016).

Sample treatment and measurements

Prior to analysis, all samples underwent a cleansing procedure to dissolve evaporitic minerals (halite, gypsum, and anhydrite). Pulverized sample material was mixed with deionized water, underwent centrifugation, and then the water was carefully pipetted off. This process was repeated three times to ensure the complete removal of all evaporitic minerals.

Subsequently, samples and standards were measured on a Kiel IV carbonate device with a Thermo Fisher MAT 253 operating in LIDI workflow at Utrecht University between August and October 2023. Samples were run in a one-to-one ratio with ETH-1, ETH-2 and ETH-3 standards (Bernasconi et al., 2021). Carbonate powder was dissolved at 70°C in 105% phosphoric acid ($H_3PO_4 + H_4P_2O_7$). The CO_2 produced in the reaction was then purified through two cryogenic (-170°C) traps and a Porapak trap (Meckler et al., 2014) kept at -40°C to -50°C.

We specifically target sabkha calcite-aragonite for clumped isotope analysis, even though some samples were calcite-dolomite mixtures (see supplementary material). Therefore, the sample carbonate powder amount required for analysis was calculated based on the XRD-derived calcite-aragonite content (Table 1). For the samples analyzed here, sample weights ranged from 180 to 480 μg (Figure S1). The reaction time of 8 minutes was chosen to ensure that the vast majority of the CO_2 produced, during this time, originated from calcite-aragonite rather than dolomite present in the fossil record. This assumption was verified by monitoring the CO_2 pressure in the bellows, which was usually within the expected range given the sample weight and calcite concentration. This monitoring ensured that the released gas was primarily derived from calcite, not dolomite (see Figure S1). Hence, the derived temperatures correspond to those at the time of the primary calcite and aragonite precipitation.

Data processing is further detailed in the supplementary material.

RESULTS AND DISCUSSION

Modern sabkha Δ_{47} measurements from the Yas Lagoon yield temperatures of 33.6 ± 6.3ºC, 33.1 ± 6.2°C and 26.2 ± 5.4ºC (2σ uncertainties, Table 1). These temperatures were calculated using the universal calibration of Anderson et al. (2021). The first two temperatures are remarkably similar, while the latter is significantly cooler, though still overlapping within their 2σ margins of error. Throughout the year, air temperatures in Abu Dhabi range from a mean minimum air temperature of 15.0°C in January to a mean maximum temperature of 40.7°C in August (Fig. 2), with an annual average of 26.8ºC. Hence, it appears that the sabkha Δ_{47}-T are too hot to reflect mean annual average temperature. Instead, the sabkha Δ_{47} temperatures correspond remarkably well with summer half-year temperatures in the area, averaging from 27.3 – 35.3° (Figure 2). These summer half-year temperatures are also in agreement with the monitored temperature at Yas lagoon itself by Lockier (2012). The interpretation of the sabkha Δ_{47} measurements as summer half-year temperatures is corroborated by sedimentological observations: These indicate that sabkhas carbonate minerals (biological/chemical) predominantly accumulate during the hot and dry season. In this part of the year, increased water evaporation rates facilitate enhanced mineral deposition (Lockier 2012).

Mid-to-Late Miocene sabkha samples from the North West Australian Shelf (IODP site U1464) yield Δ_{47}-Temperatures of 28.9 ± 6.3ºC, 31.7 ± 4.9 and 32.7 ± 4.9ºC (Table 1). These three temperatures are remarkably consistent and in the same range as the modern sabkha Δ_{47} measurements. As the modern sabkha Δ_{47} temperatures were interpreted as summer half-year temperatures, we assume a similar relationship for the Miocene samples. This interpretation is corroborated by a compilation of Miocene GCM simulations (Fig. 3). The compilation presented here, combines summer half-year temperatures (for the respective hemisphere) from the 36 model simulations in MioMIP (Burls et al., 2021) for a Middle or Late Miocene continental configuration, complemented by the three model simulation in Sarr et al. (2022). These 39 model simulations cover a vast range of atmospheric CO_2 configurations from pre-industrial 280 to 850 ppm CO_2. This wide range of CO_2 forcing in the model simulations reflects the current uncertainty on Miocene pCO2 concentrations, as well as its marked decrease from the Middle to the Late Miocene: Rae et al. (2021) reports proxy-based CO_2 reconstructions between 400 – 600 ppm. Notably, our three Middle Miocene sabkha-derived Δ_{47}-temperatures fit best with summer half-year temperatures from simulations with 350-450 ppm CO_2 (Figure 3).

Our observation that fossil and modern are characterized by rather similar sabkha summer half-year temperatures raise questions about the sensitivity of low-latitude environments to climate change. Despite significantly different atmospheric CO_2 levels between modern time and the Mid-to-Late Miocene, sabkha-derived Δ_{47}-summer-half-year temperatures seem to have remained rather similar, around 31ºC. This apparently similar sabkha temperatures between the Miocene and the recent contrast with the results of Hossain et al. (2023), who estimated Miocene global mean surface temperatures to be 3.1ºC warmer in the Miocene, at CO_2 levels of 450ppm. These lines of evidence suggest that the low latitudes were not significantly warmer compared to modern temperatures during the mid-to-late Miocene, even though the high latitudes were significantly warmer with ice-free summers in the Arctic (Stein et al., 2016). Another line of evidence for polar amplification and low-latitude attenuation of climate change is found in Herbert et al. (2016), who reported that global cooling during the Late Miocene was more pronounced in the high latitudes compared to the low latitudes, even though $U_{37}^{K`}$ sea surface temperature proxy cannot records temperatures above 28ºC.

Besides temperatures, we also infer the isotopic composition of the fluid from which sabkha formed ($\delta^{18}O_w$) by feeding measured $\delta^{18}O_{calcite}$ and Δ_{47} temperatures into the equation of Kim and O'Neal (1997). The reconstructed Mid-to-Late Miocene $\delta^{18}O_w$ values (+3.2±0.9‰ to +3.9±0.6‰) are within the expected range for an evaporative environment. For the modern sabkha samples, the calculated values range between +3.7±0.8 and +5.3±0.8‰ (Tab. 1). These values are significantly heavier than in-situ direct measurements of $\delta^{18}O_w$ values of water on the present-day Yas Lagoon sabkha (+2.2 to +3.7‰). However, we note that the present-day in-situ measurements were taken in the cool and wet season (Pederson et al., 2021), whereas we suggest the Δ_{47}-based $\delta^{18}O_w$ reconstructions to represent the warm and dry season. In other words, the heavier $\delta^{18}O_w$ isotopic compositions provide further support for our interpretation of clumped isotope temperatures as hot season temperatures. As calcite predominantly precipitated during the summer season, and with our samples originating from the most restricted part of the lagoon, calcite-derived clumped isotope temperatures likely reflect hot-season conditions with more strongly isotopically fractionated sabkha waters.

The calcite $\delta^{13}C$ and $\delta^{18}O$ values of modern and fossil sabkha samples (Table 1) are in the range of modern environment values (Pederson et al., 2021) confirming that the recorded temperatures and $\delta^{18}O_w$ refer to the precipitation of primary calcite.

Samples name	Sample	[calcite-aragonite]	Average range summer half-year T (°C)	N	Δ_{47} (‰) I-CDES	1SE	Δ_{47}-T(C°) (Anderson et al., 2021)	$\delta^{13}C$‰ (VPDB)	$\delta^{18}O$‰ (VPDB)	$\delta^{18}O_w$ ‰ (Kim et al., 1997)
MM-1	Microbial Mat	48%	27.3-35.3	23	0.574	0.0165	33.1±6.2	1.8	1.8	5.3±0.8
MM-2	Microbial Mat	87%	27.3-35.3	24	0.593	0.0163	26.2±5.4	0.6	1.5	3.7±0.8
TFM-1	Tidal Flat Mat	94%	27.3-35.3	25	0.573	0.0164	33.6±6.3	3.0	1.1	4.3±0.8
SAB-1	27R2W-29	33%		25	0.577	0.0135	31.7±4.9	2.0	0.6	3.9±0.6
SAB-2	27R2W-51	30%		23	0.586	0.0172	28.9±6.3	2.0	0.5	3.2±0.9
SAB-3	29R2W-38	90%		24	0.574	0.0132	32.7±4.9	2.4	-0.20	3.3±0.6

Table 1: Classic ($\delta^{18}O$ and $\delta^{13}C$) and clumped isotope results (Δ_{47}). Calcite-aragonite content was measured with X-Ray Diffraction (XRD, Petrick et al., 2019 for Miocene samples). Summer half-year (from April to September) temperature (https://en.climate-data.org). Δ_{47} temperatures are calculated using the unified calibration of Anderson et al., 2021, results are reported at 1SE. $\delta^{18}O_w$ values were derived using the equation of Kim and O'Neal, (1997).

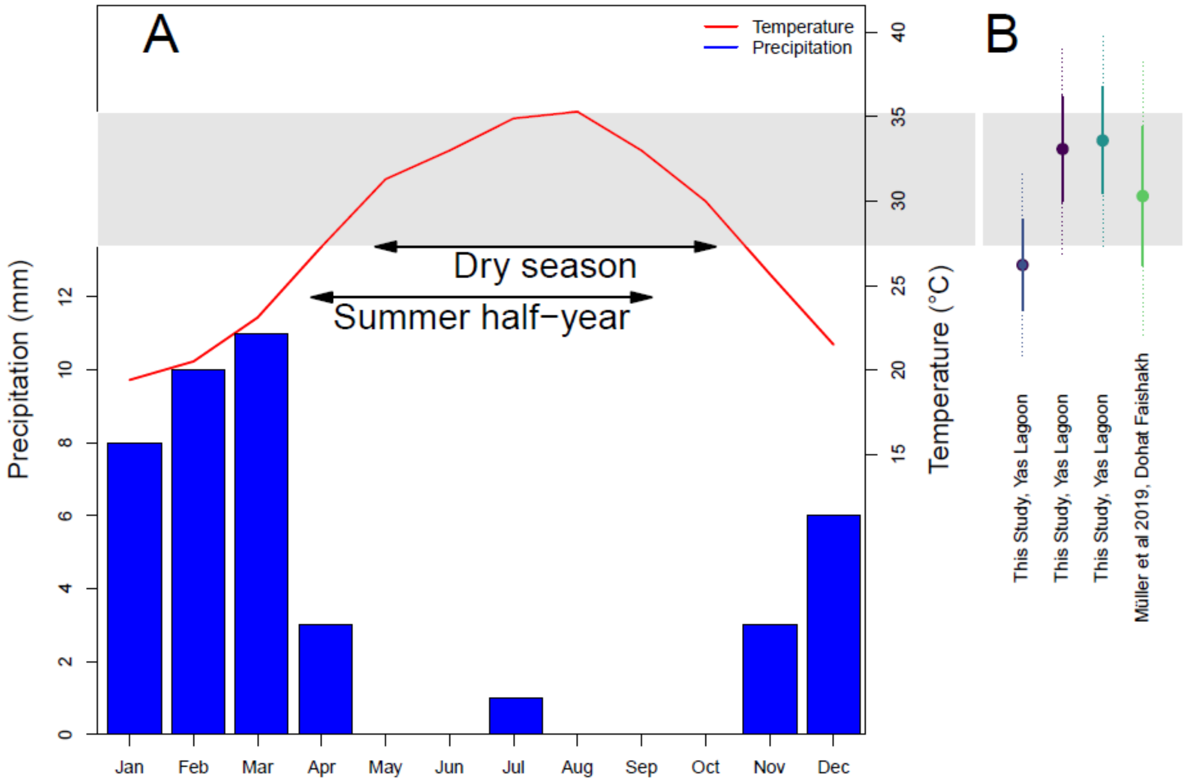

Figure 2: Δ_{47}-derived water temperatures of modern sabkha carbonates (right) align average summer half-year air temperatures in Abu Dhabi (climate graph from climate-data.org), with present-day average summer temperatures between 28 – 35°C from this study and from Müller et al., 2019.

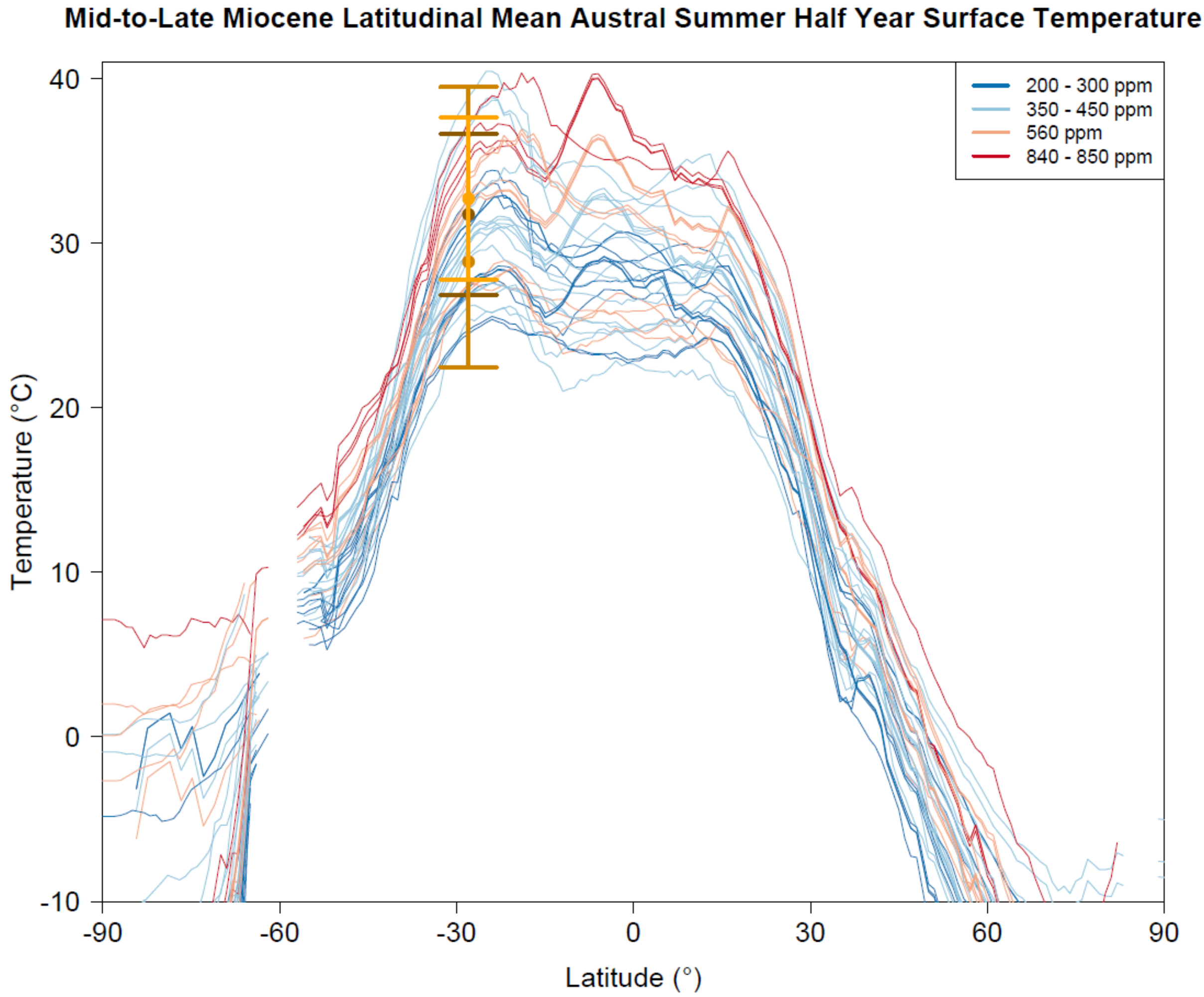

Figure 3: Δ_{47}-derived water temperatures of Middle Miocene sabkha carbonates from IODP Site U1464 (orange-brown) align with modelled summer half-year air temperatures in general circulation simulations with a Middle or Late Miocene configuration (39 model runs from MioMIP Burls et al., 2021 and Sarr et al., 2022).

CONCLUSION

Our results indicate that Mid-to-Late Miocene continental paleotemperatures at the horse latitudes were comparable to present-day conditions at similar low latitudes. This suggests that most of the changes in the global heat budget between the Miocene coolhouse and the present-day icehouse occurred in the mid to high latitudes. In other words, we found a low-latitude attenuation-in contrast to the well-documented polar amplification- of climate change.

Both modern and fossil mid-to-middle Miocene sabkha samples recorded temperatures higher than the annual air average, indicating prevalent calcite precipitation during the hottest and driest months. The reconstructed isotopic composition of the water ($\delta^{18}O_w$) suggests isotopic enrichment typical of environments with high evaporation rate.

Clumped isotopes, measured on sabkha calcite, can be used as proxy to reconstruct continental summer half-year temperatures in hot and arid environments. This approach has the potential to fill in a gap, as permanent waterbodies are very rare in the horse latitudes, and hence continental paleoclimate archives are rare as well.

ACKNOWLEDGMENTS

This research used samples and data provided by the International Ocean Discovery Program (IODP). We thank Benjamin Petrick for making his Site U1464 samples available to us, as well as for scientific discussions. We thank Nathalie Burls and Anta-Clarisse Sarr for sharing Miocene model runs and discussing their visualization. We thank Hannah Koppetz-Mitra and Theresa Block (University of Münster) for XRD analyses.

REFERENCES CITED

Abbott, S., C. M. John, and A. Fraser. "Implications of clumped-isotope thermometry for the deposition and alteration of evaporite-carbonate sabkha cycles in the Jurassic Weald Basin, UK." *AGU Fall Meeting Abstracts*. Vol. 2013. 2013.

Anderson, N. T., Kelson, J. R., Kele, S., Daëron, M., Bonifacie, M., Horita, J., et al. (2021). A unified clumped isotope thermometer calibration (0.51100° C) using carbonate-based standardization. *Geophysical Research Letters*, *48*(7), e2020GL092069. https://doi.org/10.1029/ 2020gl092069

Bergmann, K. D., Al Balushi, S. A. K., Mackey, T. J., Grotzinger, J. P., & Eiler, J. M. (2018). A 600-million-year carbonate clumped-isotope record from the Sultanate of Oman. *Journal of Sedimentary Research*, **88**(8), 960–979.

Bernasconi, S. M., Daëron, M., Bergmann, K. D., Bonifacie, M., Meckler, A. N., Affek, H. P., et al. (2021). InterCarb: A community effort to improve inter-laboratory standardization of the carbonate clumped isotope thermometer using carbonate standards. *Geochemistry, Geophysics, Geosystems*, *22*, 5. https://doi.org/10.1029/2020gc009588

Budyko, M. I. (1969). The effect of solar radiation variations on the climate of the Earth. *Tellus*, **21**, 611–619.

Burls, N. J., Bradshaw, C. D., De Boer, A. M., Herold, N., Huber, M., Pound, M., ... & Zhang, Z. (2021). Simulating miocene warmth: insights from an opportunistic multi-model ensemble (MioMIP1). *Paleoceanography and Paleoclimatology*, *36*(5), e2020PA004054.

Daëron, M., & Vermeesch, P. (2023). Omnivariant generalized least squares regression: Theory, geochronological applications, and making the case for reconciled Δ47 calibrations. *Chemical Geology*, *647*, 121881 https://doi.org/10.1016/j.chemgeo.2023.121881

Eiler, J. M. (2007). "Clumped-isotope" geochemistry—The study of naturally-occurring, multiply-substituted isotopologues. *Earth and Planetary Science Letters*, *262*(3–4), 309–327. https://doi.org/10.1016/j.epsl.2007.08.020

Fiebig, J., Daëron, M., Bernecker, M., Guo, W., Schneider, G., Boch, R., Bernasconi, S.M., Jautzy, J., Dietzel, M., 2021. Calibration of the dual clumped isotope thermometer for carbonates. Geochim. Cosmochim. Acta 312, 235–256.

Gallagher, S. J., Fulthorpe, C., Bogus, K., Heap, A., Exon, N., & Wallace, M. (2015) IODP Expedition 356: Drilling to reveal a 5 million year carbonate and subsidence history on the Northwest Shelf of Australia. doi:10.14379/iodp.proc.356.109.2017

Groeneveld, J., Henderiks, J., Renema, W., McHugh, C. M., De Vleeschouwer, D., Christensen, B. A., et al. (2017). Australian shelf sediments reveal shifts in miocene Southern hemisphere westerlies. Sci. Adv. 3:e1602567. doi: 10.1126/ sciadv.1602567

Herbert, T. D., Lawrence, K. T., Tzanova, A., Peterson, L. C., Caballero-Gill, R., & Kelly, C. S. (2016). Late Miocene global cooling and the rise of modern ecosystems. *Nature Geoscience*, **9**, 843–847. **https://doi.org/10.1029/2020PA003956**

Hossain, A., Knorr, G., Jokat, W., Lohmann, G., Hochmuth, K., Gierz, P., et al. (2023). The impact of different atmospheric CO_2 concentrations on large scale miocene temperature signatures. *Paleoceanography and Paleoclimatology*, **38**(2), e2022PA004438. **https://doi.org/10.1029/2022PA004438**

Judd, E., Tierney, J.E., Lunt, D.J., Montañez, I.P., Huber, B.T., Wing, S.L., Valdes, P.J., (2024), A 485-million-year history of Earth's surface temperature. Science, 85, eadk3705 (2024). DOI: 10.1126/science.adk3705

Kim, S. T., & O'Neil, J. R. (1997). Equilibrium and nonequilibrium oxygen isotope effects in synthetic carbonates. *Geochimica et Cosmochimica Acta*, *61*(16), 3461–3475. https://doi.org/10.1016/s0016-7037(97)00169-5

Kocsis, A. T., & Scotese, C. R. (2023). PaleoMAP PaleoCoastlines data (7.3) [Data set]. Zenodo. https://doi.org/10.5281/zenodo.7994000

Lokier, S.W. (2012) Development and evolution of subaerial halite crust morphologies in a coastal sabkha setting. *J. Arid Environ.*, **79**, 32–47.

Lokier S. W. and Fiorini F. (2016) Temporal evolution of a carbonate coastal system, Abu Dhabi, United Arab Emirates. Mar. Geol. 381, 102–113.

Müller, I. A., Rodriguez-Blanco, J. D., Storck, J.-C., do Nascimento, G. S., Bontognali, T. R. R., Vasconcelos, C., et al. (2019). Calibration of the oxygen and clumped isotope thermometers for (proto-)dolomite based on synthetic and natural carbonates. *Chemical Geology*, **525**, 1–17. **https://doi.org/10.1016/j.chemgeo.2019.07.014**

Meckler, A. N., Ziegler, M., Millan, M. I., Breitenbach, S. F. M., & Bernasconi, S. M. (2014). Long-term performance of the Kiel carbonate device with a new correction scheme for clumped isotope measurements. *Rapid Communications in Mass Spectrometry*, **28**(15), 1705–1715. **https://doi.org/10.1002/rcm.6949**

Mckenzie J., (1980) Holocene dolomitization of calcium carbonate sediments from the coastal sabkhas of Abu Dhabi, U.A.E.: a stable isotope study. The Journal of Geology, 89, 2, pp 185-198.

Nelson, J. K., Anderson, M., Bills, B., Stryker, M., Crawford, S., Blois, J., Goring, S. J., & Williams, J. W. (2023). NeotomaDB/Explorer: Neotoma Explorer Version 1.2.0. https://apps.neotomadb.org/explorer. DOI: 10.5281/zenodo.7921067.

Pederson, C. L., Ge, Y., Lokier, S. W., Swart, P. K., Vonhof, H., Strauss, H., ... & Immenhauser, A. (2021). Seawater chemistry of a modern subtropical 'epeiric'sea: Spatial variability and effects of organic decomposition. *Geochimica et cosmochimica acta*, *314*, 159-177.

Petrick, B., Reuning, L., & Martínez-García, A. (2019). Distribution of glycerol dialkyl glycerol tetraethers (GDGTs) in microbial mats from Holocene and Miocene Sabkha sediments. *Frontiers in Earth Science*, *7*, 310.

Rae, J. W., Zhang, Y. G., Liu, X., Foster, G. L., Stoll, H. M., & Whiteford, R. D. (2021). Atmospheric CO2 over the past 66 million years from marine archives. *Annual Review of Earth and Planetary Sciences*, *49*, 609-641.

Ryan, W.B.F., S.M. Carbotte, J.O. Coplan, S. O'Hara, A. Melkonian, R. Arko, R.A. Weissel, V. Ferrini, A. Goodwillie, F. Nitsche, J. Bonczkowski, and R. Zemsky (2009), Global Multi-Resolution Topography synthesis, Geochem. Geophys. Geosyst., 10, Q03014, doi:10.1029/2008GC002332.

Sarr, A. C., Donnadieu, Y., Bolton, C. T., Ladant, J. B., Licht, A., Fluteau, F., ... & Dupont-Nivet, G. (2022). Neogene South Asian monsoon rainfall and wind histories diverged due to topographic effects. *Nature Geoscience*, *15*(4), 314-319.

Sena, C.M., John, C.M., Jourdan, A.-L., Vandeginste, V. and Manning, C. (2014) Dolomitization of Lower Cretaceous pertidal carbonates by modified seawater: constraints from clumped isotopic paleothermometry, elemental chemistry, and strontium isotopes. *J. Sed. Res.*, **84**, 552–566.

Sosdian, S. M., Greenop, R., Hain, M. P., Foster, G. L., Pearson, P. N., & Lear, C. H. (2018). Constraining the evolution of Neogene ocean carbonate chemistry using the boron isotope pH proxy. Earth and Planetary Science Letters, 498, 362–376. https://doi.org/10.1016/j.epsl.2018.06.017

Stein, R., Fahl, K., Schreck, M., Knorr, G., Niessen, F., Forwick, M., et al. (2016). Evidence for ice-free summers in the late Miocene central Arctic Ocean. *Nature Communications*, **7**, 1–13. **https://doi.org/10.1038/ncomms11148**

Steinthorsdottir, M., Coxall, H. K., de Boer, A. M., Huber, M., Barbolini, N., Bradshaw, C. D., et al. (2020). The Miocene: The Future of the Past. *Paleoceanography and Paleoclimatology*, e2020PA004037.

Stendel, M., Francis, J., White, R., Williams, P. D., & Woollings, T. (2021). The jet stream and climate change. Climate change: Observed impacts on planet Earth (3rd ed., pp. 327–357). **https://doi.org/10.1016/B978-0-12-821575-3.00015-3**

Terry, J.P., Al Ruheili, A., Almarzooqi, M.A., Almheiri, R.Y. and Alshehhi, A.K., 2023. The rain deluge and flash floods of summer 2022 in the United Arab Emirates: Causes, analysis and perspectives on flood-risk reduction. *Journal of Arid Environments*, *215*, p.105013.

Warren, J.K. and Kendall, C.G.S.C., 1985. Comparison of sequences formed in marine sabkha (subaerial) and salina (subaqueous) settings—modern and ancient. *AAPG bulletin*, *69*(6), pp.1013-1023.

SUPPLEMENTARY MATERIAL

1. DATA PROCESSING

Outliers were removed from the dataset if they met one of the following criteria:

1. The intensity of the sample gas in the mass spectrometer was outside the 10 – 25 kV range.
2. The intensity on mass 49 (which is rare in natural CO_2 gases), measured as the 49/44 mass ratio relative to the working gas, exceeded 0.01‰, indicating contamination in the sample.
3. The standard deviation between Δ_{47} values calculated from different CO_2 pulses from the same sample (internal standard deviation) exceeded 0.1‰.
4. The Δ_{47}, $\delta^{18}O_c$ or $\delta^{13}C$ values measured in standard reference materials deviated significantly (>3 standard deviations) from their accepted values.

Standards and samples meeting these criteria were not considered for further analysis. Datasets from different instruments (MAT253 vs MAT253 Plus) and using different methods (LIDI vs "click-clack") were separately corrected for long-term drift by plotting the offset of standard measurements from their accepted values over time and applying a loess filter to identify trends. After correction, the external standard deviation on Δ_{47}, $\delta^{18}O_c$ or $\delta^{13}C$ values was calculated separately per instrument dataset from the independent IAEA-C2 and Merck standards before merging the datasets from both instruments.

Following the calcite-aragonite acid fractionation from Kim et al. (2007), the maximum difference between the end members of our dataset is 0.4‰. Since this value does not significantly impact our results, we conclude that no correction for acid fractionation of $\delta^{18}O_c$ is necessary. Regarding the Δ_{47} values, one sample (MM1) consists of 48% calcite and contains no aragonite. The $\delta^{18}O_c$ of this sample is 1.78‰, while two other samples (MM2 and TFM), composed of approximately 70% aragonite and 20% calcite, have $\delta^{18}O_c$ values of 1.49‰ and 1.08‰, respectively. According to Defliese and Lohmann (2015), if the difference in $\delta^{18}O_c$ between samples made of 100% calcite and 100% aragonite is less than 2‰, there is no impact on Δ_{47} values. Therefore, we conclude that no correction is needed for our Δ_{47} values.

FIGURES

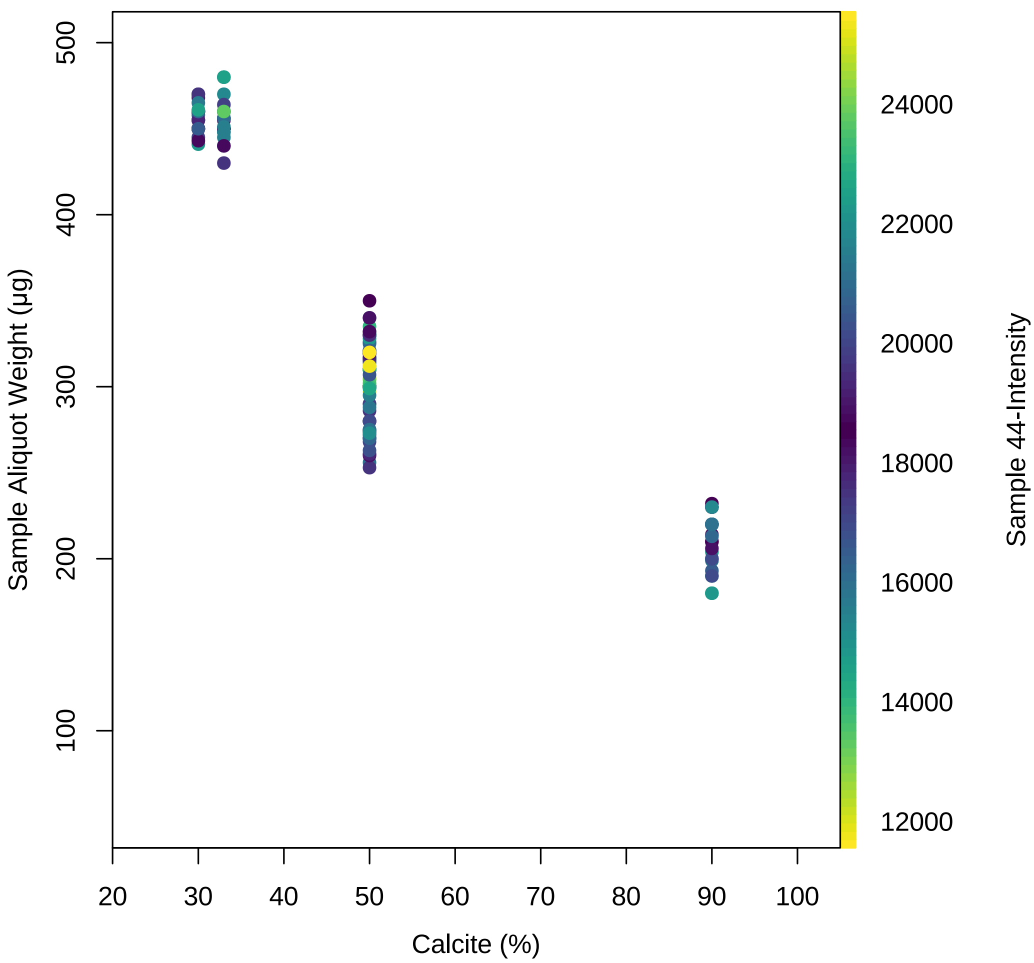

Figure S1: Comparison between sample calcite content, sample aliquote weight and sample 44-intensity. The sample 44-intenstity is usually within the expected range given the sample weight and calcite concentration. This ensured that the analysed gas is primarly derived from calcite and not dolomite.

A

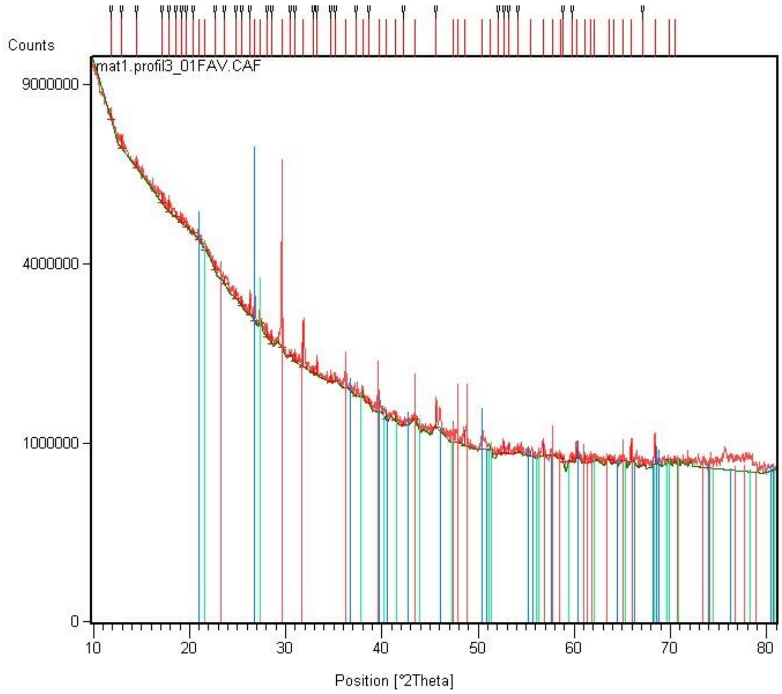
Counts
mat1.profil3_01FAV.CAF
9000000
4000000
1000000
0
10
20
30
40
50
60
70
80
Position [°2Theta]

B

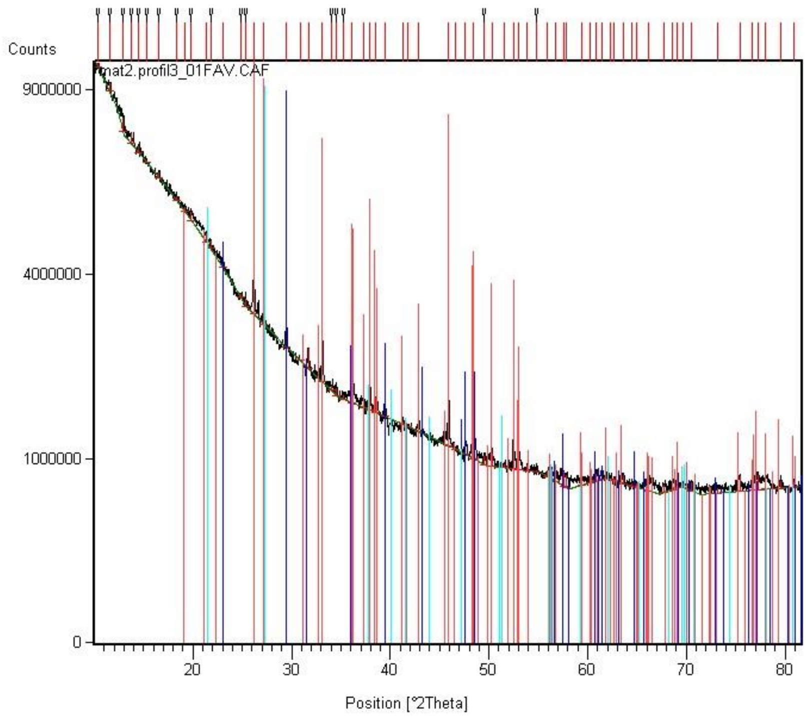
Counts
mat2.profil3_01FAV.CAF
9000000
4000000
1000000
0
20
30
40
50
60
70
80
Position [°2Theta]

C

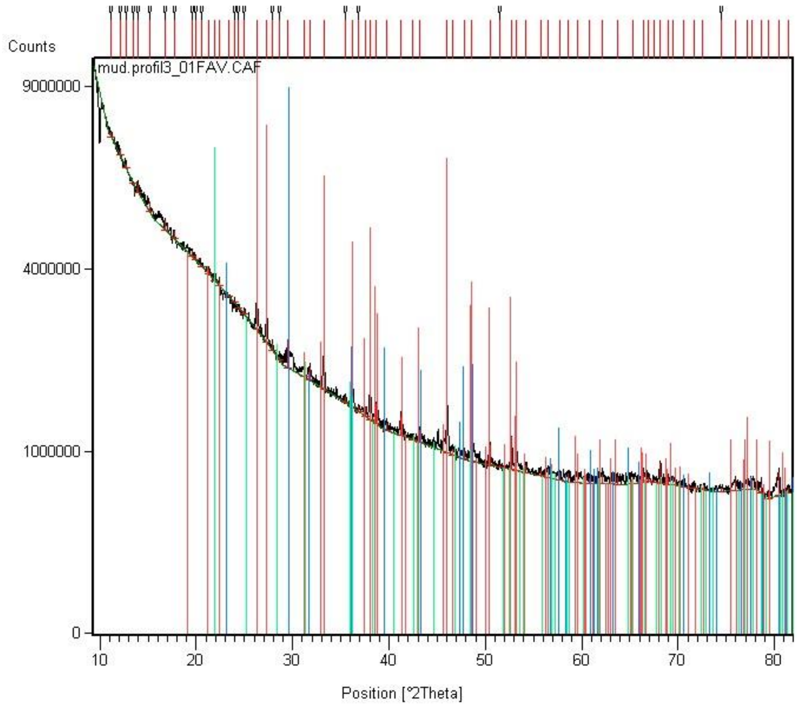

Figure 2: Results of the XRD analyses of sample MM-1 (A), MM-2 (B) and TFM-1 (C)

Table 1: XRD results

Sample Name	Nº	Compound name	Displacement [∞2Th.]	Scale Factor	RIR	SemiQuant [%]
MM-1	1	Calcite magnesian	0,048	0,434	3,050	48
	2	Quartz $GA, syn	-0,025	0,425	3,270	44
	3	Quartz	0,009	0,094	3,590	9
MM-2						
	1	Aragonite	-0,019	1,115	1,140	72
	2	Calcite	0,026	0,641	3,150	15
	3	Quartz	-0,076	0,616	3,590	13
TFM-1						
	1	Aragonite	0,087	0,933	1,140	74
	2	Magnesium calcite, syn	0,053	0,688	3,120	20
	3	Cristobalite low, syn	0,032	0,338	5,020	6

Bibliography

Defliese, W. F., & Lohmann, K. C. (2015). Non-linear mixing effects on mass-47 CO2 clumped isotope thermometry: Patterns and implications. *Rapid Communications in Mass Spectrometry*, 29(9), 901–909. https://doi.org/10.1002/rcm.7175

Kim S.-T., Mucci A. and Taylor B. E. (2007) Phosphoric acid fractionation factors for calcite and aragonite between 25 and 75 °C: revisited. Chem. Geol. 246, 135–146.